Biochemical and Biophysical Research Communications 394 (2010) 94–99

Contents lists available at ScienceDirect

Biochemical and Biophysical Research Communications

journal homepage: www.elsevier.com/locate/ybbrc

Direct measurement of shear strain in adherent vascular endothelial cells exposed to fluid shear stress

Yosuke Ueki [a,b,*], Naoya Sakamoto [a], Masaaki Sato [a,c]

[a] Department of Bioengineering and Robotics, Graduate School of Engineering, Tohoku University, Japan
[b] Research Fellow of the Japan Society for the Promotion of Science, Japan
[c] Department of Biomedical Engineering, Graduate School of Biomedical Engineering, Tohoku University, Japan

ARTICLE INFO

Article history:
Received 17 February 2010
Available online 20 February 2010

Keywords:
Endothelial cell
Fluid shear stress
Shear modulus
Force transmission
Confocal microscopy

ABSTRACT

Functional and morphological responses of endothelial cells (ECs) to fluid shear stress are thought to be mediated by several mechanosensitive molecules. However, how the force due to fluid shear stress applied to the apical surface of ECs is transmitted to the mechanosensors is poorly understood. In the present paper, we performed an analysis of an intracellular mechanical field by observation of the deformation behaviors of living ECs exposed to shear stress with a novel experimental method. Lateral images of human umbilical vein ECs before and after the onset of flow were obtained by confocal microscopy, and image correlation and finite element analysis were performed for quantitative analyses of subcellular strain due to shear stress. The shear strain of the cells changed from 1.06 ± 1.09% (mean ± SD) to 4.67 ± 1.79% as the magnitude of the shear stress increased from 2 to 10 Pa. The nuclei of ECs also exhibited shear deformation, which was similar to that observed in cytoplasm, suggesting that nuclei transmit forces from apical to intracellular components, as well as cytoskeletons. The obtained strain–stress relation resulted in a mean shear modulus of 213 Pa for adherent ECs. These results provide a mechanical perspective on the investigation of flow-sensing mechanisms of ECs.

1. Introduction

Hemodynamic fluid shear stress (FSS) acting on vascular endothelial cells (ECs) evokes a variety of cellular responses, including proliferation [1], expression of adhesive molecules [2], cytoskeletal structures and morphology [3], and mechanical properties [4] that may be relevant to both the physiology and pathology of blood vessels. Thus, numerous previous studies have attempted to determine the mechanism by which ECs sense FSS and adapt to mechanical environments. Recently, FSS-induced activation of several of the candidate mechanosensitive molecules, such as G proteins [5] and PECAM-1 [6], has been demonstrated. However, as of yet, there is no primary evidence as to whether these molecules are activated directly by mechanical loading or by intracellular signaling interactions that were cued by another mechanosensor. This is thought to be due to the difficulties in precisely describing the intracellular mechanical conditions, i.e., how FSS acting on the apical surface of ECs is transmitted and generates an intracellular mechanical field. As such, it is necessary to investigate the degree to which forces are exerted on the intercellular junction, focal adhesions, and other candidates for mechanotransducers.

Helmke et al. [7,8] reported the flow-induced displacement of intermediate filaments downstream of the flow and calculated the intracellular strain field from movements of cytoskeletal networks. However, they could not clearly distinguish the passive deformation of cells from the active response of cells via biochemical responses. This may be one of the difficulties in experimentally revealing the mechanism of FSS-sensing by ECs. Numerical approaches are efficient methods by which to overcome the difficulty of separating passive deformation from active cell movements. Some previous reports have used computational analysis to evaluate the mechanical environment of ECs exposed to FSS [9,10]. Ferko et al. [10] reported a method for analyzing the intracellular strain fields of ECs exposed to shear flow using a cell-specific finite element model, in which the subcellular structures of the nucleus and focal adhesions were incorporated. However, these computational studies could not reveal the actual intracellular mechanical environment at the subcellular level because living cells have more complicated internal structures, such as cytoskeletons, which may contribute to intercellular force transmission and mechanical properties [11,12]. In addition, the actual shear modulus of cells, which is a critical determinant of the shear-induced deformation of cells, is thought to be different from the theoretical value

* Corresponding author. Address: Department of Bioengineering and Robotics, Graduate School of Engineering, Tohoku University, 6-6-01, Aramaki-aoba, Aoba-ward, Sendai City, Japan. Fax: +81 22 795 6945.
E-mail address: ueki@bml.mech.tohoku.ac.jp (Y. Ueki).

0006-291X/$ - see front matter © 2010 Elsevier Inc. All rights reserved.
doi:10.1016/j.bbrc.2010.02.115

computed from Young's modulus with the assumptions of isotropy and incompressibility, while the modulus has been used in almost all computational studies.

In an attempt to solve this problem, in the present study, we report a novel experimental technique that enables direct observation of the passive deformation of living ECs exposed to the physiological range of FSS by confocal microscopy and the measurement of the intracellular strain field together with the application of image processing and the finite element method (FEM). To reveal the role of actin filaments in force bearing in ECs exposed to FSS, the deformation behavior of ECs treated with cytochalasin D is also analyzed. In addition, we calculate the shear modulus of ECs and measure the shear strain of ECs exposed to FSS controlled to physiological magnitudes.

2. Materials and methods

2.1. Cell culture and fluorescent labeling

Human umbilical vein endothelial cells (HUVECs) isolated from umbilical veins by trypsin treatment, as described in a previous study [13], were grown in Medium 199 (Invitrogen) containing 20% fetal bovine serum (JRH Biosciences), 10 ng/ml basic fibroblast growth factor (Austral Biologicals), and penicillin–streptomycin (Invitrogen). For the experiment, cells were seeded on a ϕ35-mm glass-bottom dish (with a ϕ12-mm hole on the bottom and covered with a ϕ27-mm cover glass, AGC Techno Glass) pre-coated with 0.1% bovine gelatin (Sigma–Aldrich). The following experiments were conducted after the cells achieved confluence.

Two hours before the experiment, the cytoplasmic domain and nuclei of living HUVECs were stained with 10 μM Cell Tracker Red CMTPX (Invitrogen) and 5 μM SYTO13 (Invitrogen), respectively. These fluorescent dyes induced speckled patterns of labeling, which are suitable for the image correlation described later herein.

In order to evaluate the role of actin cytoskeletons in FSS-induced deformations, HUVECs were treated with 0.2 or 2 μM cytochalasin D (CytoD, Enzo Life Sciences), which is a commonly used regent for the inhibition of actin polymerization, for 30 min prior to the experiments.

2.2. Experimental setup and procedure

The flow-exposure system consisting of a parallel plate flow chamber, a syringe pump (KDS210, KD Scientific), a tube heater (MATS-TH, Tokai hit), and polyethylene tubes (Imamura) was used in the present study (Fig. 1). The flow chamber was composed of a cell culture dish, a polycarbonate I/O unit, and a silicone gasket, which determines the geometry of the flow section of 0.2 mm in height and 2 mm in width. The mean shear stress acting on the HUVEC monolayer is expressed as

$$\tau = 6\mu Q/bh^2, \quad (1)$$

where μ is the viscosity of the culture medium, which was 0.74 mPa s (at 37 °C) as measured with a sine wave vibro-viscometer (SV10, A&D), Q is the flow rate, and h and b are the flow channel height and width, respectively. The flow rate driven by the pump was controlled to expose the HUVEC monolayer to FSS of desired magnitudes. To maintain the appropriate pH during the experiments in a low CO_2 atmosphere (room atmosphere), the medium was replaced into M199 with Hanks' salts (Invitrogen). For the CytoD-treated experiment, the same concentration of CytoD used to pre-treat the HUVECs was added to the medium. The chamber was mounted on a stage equipped with a thermo-control system (MI-IBC, Olympus) of an inverted confocal laser scanning microscope (CLSM, FV1000, Olympus). The temperature of the medium was maintained at between 35 and 37 °C by means of the tube heater and the thermo-control system. Lateral images of HUVECs were obtained using a 100× objective lens (UplanApo, NA = 1.35, Olympus) in line scanning mode at a pixel resolution of 124 nm/pixel and a vertical spacing of 120 nm/pixel. Based on the Rayleigh criterion, the optical horizontal resolution was 226 nm at a wavelength of 500 nm. The image size was approximately 1000 pixels (horizontal) × 150 pixels (vertical), and the time required for scanning was 3–4 s/frame. The scanning line was set to be parallel to the direction of flow crossing the vicinity of the center of the nucleus and containing two to four HUVECs in one frame. A personal computer (NJ2150, Epson Direct) with a custom Labview 8.6 (National Instruments) program was used to synchronize the pushing motion of the syringe pump and the trigger signal for image acquisition by CLSM for a temporally well-coordinated measurement.

Fig. 1B shows the experimental regime for measurements of cell deformation. Based on the intracellular stress tomography reported by Hu et al. [11], we used intermittent patterns of FSS exposure and image acquisition, which was phase-locked to the periodic FSS exposure, for precise measurement of the intracellular mechanical field. The square-wave form pattern of FSS with a frequency of 0.05 Hz, which corresponds to the alternating repetition of a 10 s FSS exposure and a 10 s pause of FSS, were applied to ECs. Trigger signals for image acquisition were input to the CLSM at 5 s after onset and offset of flow. This 20 s cycle of flow pattern and image acquisition was repeated five times at the same FSS level. Therefore, we obtained five "deformed" and five "undeformed" lateral images of HUVECs. This procedure facilitated the reduction of the effect of random movement of intracellular structures and active deformation of cells due to cell migration. This five-cycle repetition was performed sequentially while varying the maximum FSS as 2, 4, 6, and 10 Pa, so that the deformation of identical cells could be measured under various shear stress levels.

2.3. Image correlation

To obtain the intracellular displacement field, an image correlation analysis was carried out between the undeformed and deformed images. Prior to the analysis, the following image processing was performed using ImageJ 1.40b software (National Institutes of Health). First, the parallel displacement in the vertical direction of the cells in the lateral images were corrected because the change in internal pressure of the chamber due to flow induced the deflection of the glass bottom, resulting in a vertical shift of the images. The center-of-mass of the cross section of the cells was detected with the "Analyze particle" function of ImageJ. Based on these obtained drift data, the vertical positions of the images were corrected using the "Translate" function of ImageJ with sub-pixel interpolation. Then, the aspect ratio of the images was corrected from 0.124:0.120 (horizontal:vertical) to 1:1. Finally, the averaged images were generated from "deformed" and "undeformed" images, respectively, using the image calculation function of ImageJ in order to reduce the noise.

Displacement vectors of each pixel in lateral images were obtained from a pair of averaged "deformed" and "undeformed" images with an image correlation method using Flow-vec 2.8 software (Library). A small region of 13 × 13 pixels surrounding the object pixel was set as the sample window. The displacement of each window was detected with a spatial resolution of approximately 1/10 pixel, corresponding to approximately 12 nm.

2.4. FEM analysis

FEM analysis was performed to calculate the strain field from the displacement field using ANSYS 11.0 multipurpose FEM analysis software (ANSYS). Conversion of image data to the finite element model was performed as follows. All pixels in an image

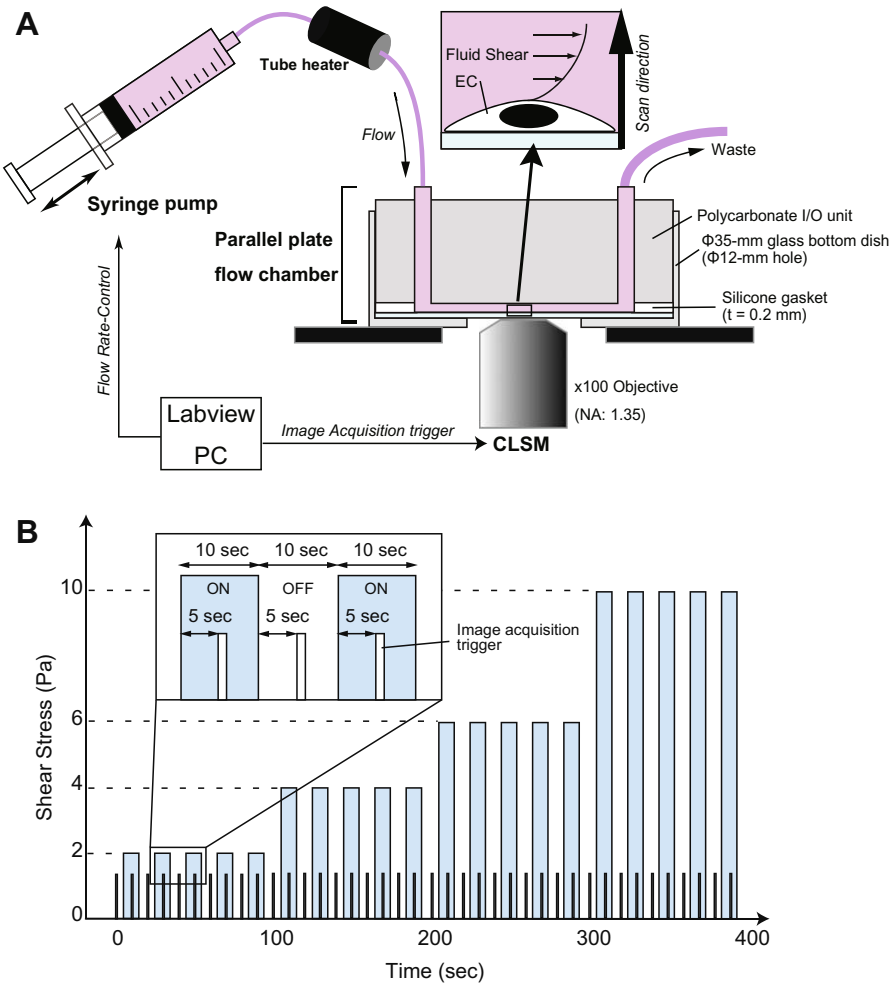

Fig. 1. Experimental setup and procedure. (A) Schematic diagram of the experimental setup for visualization of FSS-induced deformation of ECs. A parallel plate flow chamber is illustrated in a cross-sectional view. (B) Diagram of the experimental regime. A HUVEC monolayer was exposed to square-wave form FSS with a frequency of 0.05 Hz, a duty cycle of 50%, and amplitudes of 2, 4, 6, and 10 Pa.

were converted into nodes of four-node shell elements in FEM, and the vectors obtained from image correlation were allocated to nodes as constraint displacements. After the obtaining the solution, we obtained the shear strain in each pixel as nodal solutions.

2.5. Calculation of shear modulus

To calculate the shear modulus of adherent HUVECs, the mean shear strain of a cell was calculated by averaging the shear strains of all pixels on the cells. Therefore, the shear modulus (G) can be calculated using following simple equation, which is the definition of shear modulus:

$$\tau = G\gamma, \tag{2}$$

where τ is the applied FSS and γ is the mean shear strain.

3. Results and discussion

3.1. FSS-induced deformation of ECs

In the present study, we observed the deformation of ECs exposed to FSS by confocal microscopy. As shown in Movie S1 (in Supplementary material), we successively observed the deformation behavior of ECs under a shear stress of 2–10 Pa. Fig. 2 shows representative lateral views of fluorescent images of ECs (Fig. 2A–H), displacement fields (Fig. 2I–L), and shear strain fields (Fig. 2M–P). As shown in Fig. 2I–L (particularly clearly in Fig. 2K and L), large displacements (of up to 600 nm) were observed at the apical side of the cells, whereas the displacements of the bottom sides were small compared to the apical side. The difference in displacement between the apical and basal sides provides a direct indication of the shear deformation of cells. To our knowledge, this is the first report of the direct measurement of shear deformation of adherent ECs exposed to FSS. Helmke et al. [7,8] observed the FSS-induced deformation of ECs using an experimental procedure similar to that of the present study. They analyzed the total passive and active cell deformation that occurred 3 min after flow onset. On the other hand, in the present study, from the total deformation, we extracted only the displacements due to passive deformation that occurred 10 s after flow onset. Therefore, to our knowledge, the observation of the present study is the first to distinguish passive deformation from the active responses of ECs exposed to FSS.

As shown in Fig. 2A through, the greater part of the lateral images of the HUVECs was occupied by nuclei, and the shear deformation of the cell was accompanied by deformation of the nucleus (Fig. 2E–H, Movie S1). The shear strain mappings shown in Fig. 2M–P had scattered distributions, and no difference in the magnitude of shear strain between the cytoplasm and the nuclei was observed. According to previous reports [14,15], the nucleus is approximately 2.5–16 times stiffer than the cytoplasm. These results suggest the existence of mechanical connections between the

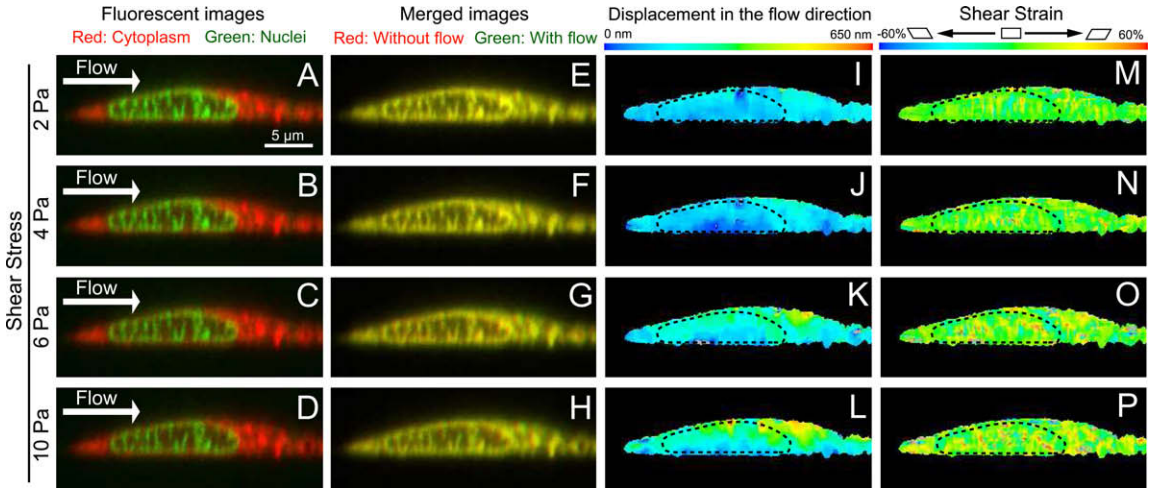

Fig. 2. Lateral images of HUVECs exposed to FSSs of 2 Pa (A, E, I, and M), 4 Pa (B, F, J, and N), 6 Pa (C, G, K, and O), and 10 Pa (D, H, L, and P). (A–D) Fluorescent images of nuclei (green) and cytoplasm (red) of HUVECs under given FSS. (E–H) Merged images of HUVECs under static (red) and flow (green) conditions. Disagreement of green and red colors indicates the displacement due to the flow. (I–L) Contour mappings of displacement in the flow direction. (M–P) Contour mappings of shear strain analyzed using FEM. The dextral and sinistral shear strains are indicated by warm and cold colors, respectively. (For interpretation of the references to color in this figure legend, the reader is referred to the web version of this paper.)

apical surface and the basal side via the nucleus transmitting forces. Crisp et al. [16] reported a structural linkage between the actin cytoskeleton and the nuclei via nesprin molecules, and Wang et al. [17] suggested that this connection contributes to the force transmission from the extracellular matrix to the nuclei. Taken together, the nucleus can act not only as a mechanosensor but also as a force transmitter as well as a cytoskeletal structure [11], which is known to transmit forces on the apical surface to focal adhesions containing several candidate mechanosensitive molecules.

3.2. Shear modulus of HUVECs

The mean shear strain level in each cell was increased proportional to the magnitude of FSS applied, as indicated in Fig. 3. The shear strain was 1.03 ± 1.09% (mean ± SD) at 2 Pa and increased to 4.67 ± 1.79% at 10 Pa. These values correspond to shear angles of 0.59° and 2.67°, respectively. From the linear relationship between the applied FSS (τ) and the shear strain (γ), we obtained following relationship:

$$\gamma\ [\%] = 1/G \cdot 100 \cdot \tau = 0.469 \cdot \tau\ [\mathrm{Pa}]. \quad (3)$$

Then, the shear modulus (G) of HUVECs is expressed as follows:

$$G = 1/0.469 \cdot 100 = 213\ [\mathrm{Pa}]. \quad (4)$$

We can also obtain the shear modulus of the cell from Young's modulus (E) from the following equation under the assumptions of incompressibility and isotropy, as follows:

$$G = E/2(1+\nu), \quad (5)$$

where ν is Poisson's ratio. Under the assumption of incompressibility ($\nu = 0.5$), we obtain:

$$G = E/3. \quad (6)$$

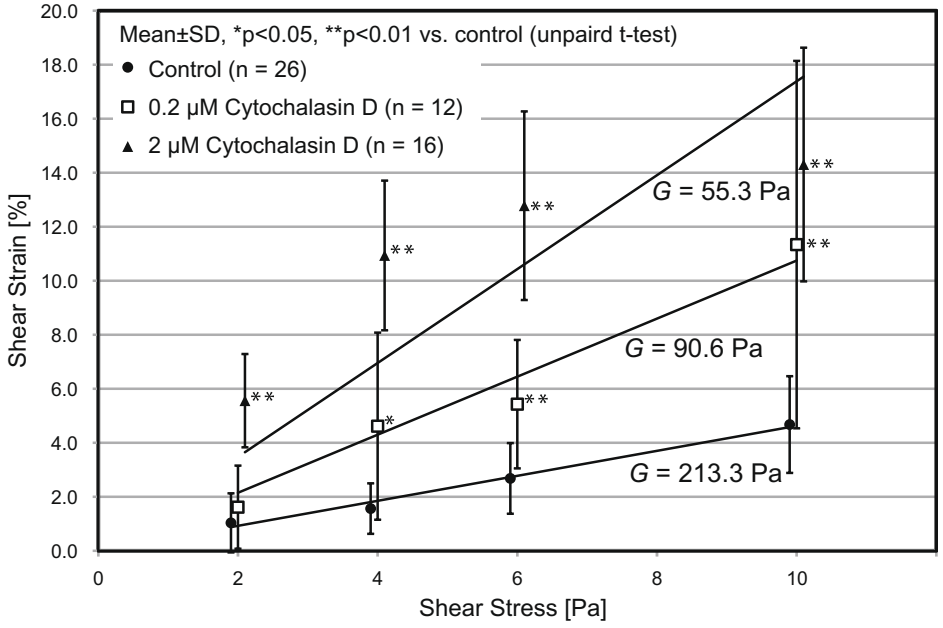

Fig. 3. Relationship between the applied FSS and the shear strain of HUVECs. Control cells (closed circles), 0.2 μM CytoD treated cells (open squares), and 2 μM CytoD treated cells (closed triangles).

Kataoka et al. [18] and Mathur et al. [14] measured the Young's modulus of HUVECs by indentation measurement using atomic force microscope (AFM) and reported the Young's modulus to be in the range of 3–6 kPa, which, based on Eq. (6), yields a shear modulus in the range of from 1 to 2 kPa. Therefore, the shear modulus obtained in the present study is considered to be smaller than the value calculated from the previously reported Young's modulus under the assumptions of incompressibility and isotropy. Although the reason for this difference is unclear, a number of possibilities have been suggested. First, the limitation of the assumption of isotropy has been suggested to induce the difference in the values. Hu et al. [19] reported that the anisotropic mechanical property of adherent cells depends on actin cytoskeletons. Second, we calculated the shear modulus under the assumption that the average shear stresses of 2, 4, 6, and 10 Pa induced shear strain in the ECs. However, it has been reported that shear stresses acting on the EC surface are nonuniformly distributed, depending on the surface topography of ECs, and that a maximum shear stress greater than mean is exerted at the apex of ECs [10,20]. In the present study, we averaged the shear strain in each pixel of a cell in calculating the mean shear strain in a cell. If FSS increases at the apex region of ECs, the mean shear strain may have been overestimated because the local strain beneath the apex region, which occupies a large part of the vertical section of the ECs, would be much larger than the other part of the ECs and would have a significant effect on the mean value. Furthermore, the heterogeneity of the cell is thought to be the reason for this difference. Previous studies reporting the Young's modulus of HUVECs have used AFM. The Young's modulus obtained by AFM may be affected by the local stiffness of the cell surface, which contains a stiff cortical layer consisting primarily of actin filaments. On the other hand, the shear modulus presented in the present study is calculated from the strain over the entire area of the HUVEC.

3.3. Role of actin filaments in FSS-induced deformation

Fig. 4G–L and M–R shows the displacement fields and shear strain fields, respectively, of HUVECs treated with CytoD. Both displacement and shear strain increased with the increase in CytoD concentration. The maximum displacement was more than 2 μm, and the maximal shear strain exceeded 50% (both indicated in gray in the contour images) in the HUVECs treated using 2 μM CytoD exposed to 10 Pa. As shown in Fig. 3, the shear strain caused by FSS of the ECs increased significantly upon CytoD treatment. The shear moduli of HUVECs treated with 0.2 and 2 μM CytoD were 90.6 and 55.3 Pa, respectively. Wakatsuki et al. [21] reported the relationship between the normal stiffness of cells measured by indentation testing and the concentration of treated CytoD. According to their report, the normal stiffness decreased to approximately 40% and 15% when cells were treated with 0.2 μM CytoD and 2 μM CytoD, respectively. In the present study, treatment with CytoD of the same concentrations reduced the shear moduli to 42% and 25%, respectively. This result suggests that actin cytoskeleton contributes to the shear force bearing as well as the normal force.

Some previous studies have reported polarized biochemical responses in ECs exposed to FSS [22,23]. For example, Zaidel-Bar et al. [22] reported that FSS induces phosphorylation of paxillin at the downstream edge and inactivation of small GTPase Rac1 at the upstream side of ECs. In addition, we previously suggested that the directional remodeling of ECs are mediated by activation of mechanosensors in the localized region of a cell [24]. Taken together, locally concentrated forces are considered to be exerted on mechanosensors to induce the localized activation of the signal transduction leading to the directional remodeling of cells. Recent reports have suggested that the locally applied force transmitted through cytoskeletons induces rapid activation of Rac1 at the distal point from the point of application of the force [25], which suggests that force transmission via cytoskeletons may play an important role in the polarized activation of mechanosensors. However, in the present study, we did not investigate force transmission to an extracellular matrix or to adjacent cells. According to these findings and considerations, further investigations should include quantitative evaluations of force transmission to the candidates for mechanosensors, such as focal adhesions or intercellular junctions, and localized biological responses such as the activation of RhoGTPases [22,23,25] in order to demonstrate the correlation be-

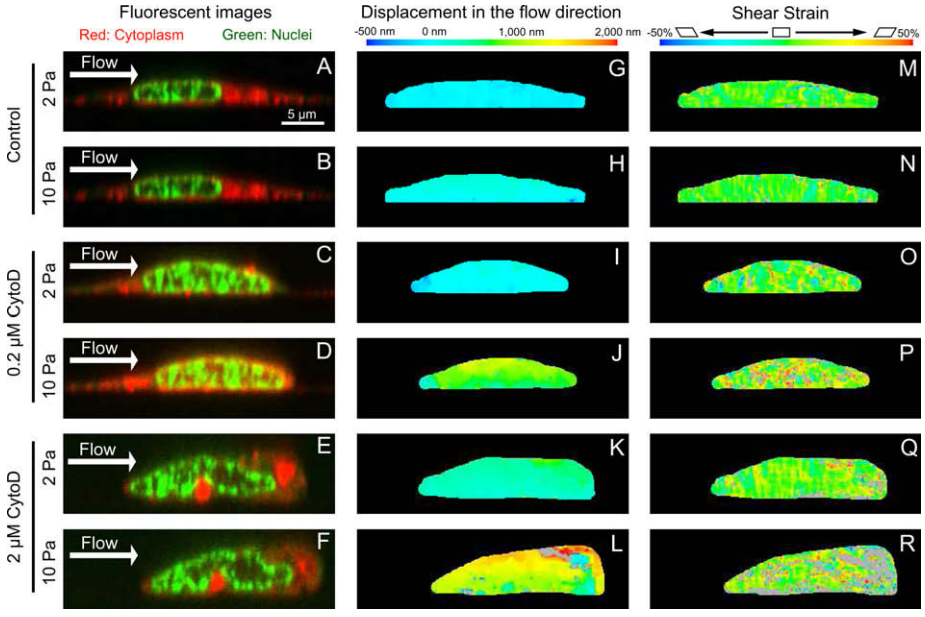

Fig. 4. Lateral images of HUVECs exposed to FSSs of 2 Pa (A, G, M, C, I, O, E, H, and Q) and 10 Pa (B, H, N, D, J, P, F, L, and R). (C, D, I, J, O, and P) HUVECs treated with 0.2 μM CytoD, and (E, F, K, L, Q, and R) HUVECs treated with 2 μM CytoD. (A–F) Fluorescent images of nucleus (green) and cytoplasm (red) of HUVECs under a given FSS. (G–L) Contour mapping of the displacement to the flow direction (left to right). (M–R) Contour mapping of the shear strain. The dextral and sinistral shear, strains are indicated by warm and cold colors, respectively. (For interpretation of the references to color in this figure legend, the reader is referred to the web version of this paper.)

tween mechanical fields and mechanotransduction in ECs exposed to FSS.

4. Conclusion

In the present study, we proposed a novel but simple technique to observe the passive shear deformation of living ECs exposed to FSS of physiological levels. Using image correlation and FEM analysis, we analyzed the subcellular strain field of ECs quantitatively and calculated the shear modulus of adherent ECs without any contacting probes. As a result, ECs and their nuclei were demonstrated to exhibit shear strain proportional to the applied FSS and the shear modulus of ECs was found to be 213 Pa.

Acknowledgments

The authors thank Dr. Ikuo Takahashi for kindly providing the human umbilical cords with the informed consent of donors. The present study was supported in part by Grants-in-Aid for Scientific Research from the Ministry of Education, Culture, Sports, Science and Technology (MEXT) of Japan (Nos. 20001007 and 21-3835).

Appendix A. Supplementary data

Supplementary data associated with this article can be found, in the online version, at doi:10.1016/j.bbrc.2010.02.115.

References

[1] M.J. Levesque, R.M. Nerem, E.A. Sprague, Vascular endothelial cell proliferation in culture and the influence of flow, Biomaterials 11 (1990) 702–707.
[2] M. Morigi, C. Zoja, M. Figliuzzi, M. Foppolo, G. Micheletti, M. Bontempelli, M. Saronni, G. Remuzzi, A. Remuzzi, Fluid shear stress modulates surface expression of adhesion molecules by endothelial cells, Blood 85 (1995) 1696–1703.
[3] C.G. Galbraith, R. Skalak, S. Chien, Shear stress induces spatial reorganization of the endothelial cell cytoskeleton, Cell Motil. Cytoskeleton 40 (1998) 317–330.
[4] M. Sato, K. Nagayama, N. Kataoka, M. Sasaki, K. Hane, Local mechanical properties measured by atomic force microscopy for cultured bovine endothelial cells exposed to shear stress, J. Biomech. 33 (2000) 127–135.
[5] S.R. Gudi, C.B. Clark, J.A. Frangos, Fluid flow rapidly activates G proteins in human endothelial cells. Involvement of G proteins in mechanochemical signal transduction, Circ. Res. 79 (1996) 834–839.
[6] E. Tzima, M. Irani-Tehrani, W.B. Kiosses, E. Dejana, D.A. Schultz, B. Engelhardt, G. Cao, H. DeLisser, M.A. Schwartz, A mechanosensory complex that mediates the endothelial cell response to fluid shear stress, Nature 437 (2005) 426–431.
[7] B.P. Helmke, D.B. Thakker, R.D. Goldman, P.F. Davies, Spatiotemporal analysis of flow-induced intermediate filament displacement in living endothelial cells, Biophys. J. 80 (2001) 184–194.
[8] B.P. Helmke, A.B. Rosen, P.F. Davies, Mapping mechanical strain of an endogenous cytoskeletal network in living endothelial cells, Biophys. J. 84 (2003) 2691–2699.
[9] T. Ohashi, H. Sugawara, T. Matsumoto, M. Sato, Surface topography measurement and intracellular stress analysis of cultured endothelial cells exposed to fluid shear stress, JSME Int. J. C Mech. Syst. Mach. Elem. Manuf. 43 (2000) 780–786.
[10] M.C. Ferko, A. Bhatnagar, M.B. Garcia, P.J. Butler, Finite-element stress analysis of a multicomponent model of sheared and focally-adhered endothelial cells, Ann. Biomed. Eng. 35 (2007) 208–223.
[11] S. Hu, J. Chen, B. Fabry, Y. Numaguchi, A. Gouldstone, D.E. Ingber, J.J. Fredberg, J.P. Butler, N. Wang, Intracellular stress tomography reveals stress focusing and structural anisotropy in cytoskeleton of living cells, Am. J. Physiol. Cell Physiol. 285 (2003) C1082–C1090.
[12] M. Sato, K. Suzuki, Y. Ueki, T. Ohashi, Microelastic mapping of living endothelial cells exposed to shear stress in relation to three-dimensional distribution of actin filaments, Acta Biomater. 3 (2007) 311–319.
[13] N. Sakamoto, T. Ohashi, M. Sato, Effect of magnetic field on nitric oxide synthesis of cultured endothelial cells, Int. J. Appl. Electromagn. Mech. 14 (2001) 317–322.
[14] A.B. Mathur, G.A. Truskey, W.M. Reichert, Atomic force and total internal reflection fluorescence microscopy for the study of force transmission in endothelial cells, Biophys. J. 78 (2000) 1725–1735.
[15] N. Caille, O. Thoumine, Y. Tardy, J.-J. Meister, Contribution of the nucleus to the mechanical properties of endothelial cells, J. Biomech. 35 (2002) 177–187.
[16] M. Crisp, Q. Liu, K. Roux, J.B. Rattner, C. Shanahan, B. Burke, P.D. Stahl, D. Hodzic, Coupling of the nucleus and cytoplasm: role of the LINC complex, J. Cell Biol. 172 (2006) 41–53.
[17] N. Wang, J.D. Tytell, D.E. Ingber, Mechanotransduction at a distance: mechanically coupling the extracellular matrix with the nucleus, Nat. Rev. Mol. Cell Biol. 10 (2009) 75–82.
[18] N. Kataoka, K. Iwaki, K. Hashimoto, S. Mochizuki, Y. Ogasawara, M. Sato, K. Tsujioka, F. Kajiya, Measurements of endothelial cell-to-cell and cell-to-substrate gaps and micromechanical properties of endothelial cells during monocyte adhesion, Proc. Natl. Acad. Sci. USA 99 (2002) 15638–15643.
[19] S. Hu, L. Eberhard, J. Chen, J.C. Love, J.P. Butler, J.J. Fredberg, G.M. Whitesides, N. Wang, Mechanical anisotropy of adherent cells probed by a three-dimensional magnetic twisting device, Am. J. Physiol. Cell Physiol. 287 (2004) C1184–C1191.
[20] T. Yamaguchi, Y. Yamamoto, H. Liu, Computational mechanical model studies on the spontaneous emergent morphogenesis of the cultured endothelial cells, J. Biomech. 33 (2000) 115–126.
[21] T. Wakatsuki, B. Schwab, N.C. Thompson, E.L. Elson, Effects of cytochalasin D and latrunculin B on mechanical properties of cells, J. Cell Sci. 114 (2001) 1025–1036.
[22] R. Zaidel-Bar, Z. Kam, B. Geiger, Polarized downregulation of the paxillin-p130CAS-Rac1 pathway induced by shear flow, J. Cell Sci. 118 (2005) 3997–4007.
[23] E. Tzima, M.A. Del Pozo, W.B. Kiosses, S.A. Mohamed, S. Li, S. Chien, M.A. Schwartz, Activation of Rac1 by shear stress in endothelial cells mediates both cytoskeletal reorganization and effects on gene expression, EMBO J. 21 (2002) 6791–6800.
[24] Y. Ueki, N. Sakamoto, T. Ohashi, M. Sato, Morphological responses of vascular endothelial cells induced by local stretch transmitted through intercellular junctions, Exp. Mech. 49 (2009) 125–134.
[25] Y.C. Poh, S. Na, F. Chowdhury, M. Ouyang, Y. Wang, N. Wang, Rapid activation of Rac GTPase in living cells by force is independent of Src, PLoS One 4 (2009) e7886.